

Experimental generation of 6 dB continuous variable entanglement from a nondegenerate optical parametric amplifier

Yu Wang, Heng Shen, Xiaoli Jin, Xiaolong Su,* Changde Xie, and Kunchi Peng

State Key Laboratory of Quantum Optics and Quantum Optics Devices, Institute of Opto-Electronics, Shanxi University, Taiyuan, 030006, People's Republic of China

*suxl@sxu.edu.cn

Abstract: We experimentally demonstrated that the quantum correlations of amplitude and phase quadratures between signal and idler beams produced from a non-degenerate optical parametric amplifier (NOPA) can be significantly improved by using a mode cleaner in the pump field and reducing the phase fluctuations in phase locking systems. Based on the two technical improvements the quantum entanglement measured with a two-mode homodyne detector is enhanced from ~ 4 dB to ~ 6 dB below the quantum noise limit using the same NOPA and nonlinear crystal.

© 2010 Optical Society of America

OCIS codes: (270.0270) Quantum optics; (270.6570) Squeezed states

References and links

1. A. Furusawa, J. L. Sørensen, S. L. Braunstein, C. A. Fuchs, H. J. Kimble, and E. S. Polzik, "Unconditional Quantum Teleportation," *Science* **282**, 706–709 (1998).
2. H. Yonezawa, T. Aoki, and A. Furusawa, "Demonstration of a quantum teleportation network for continuous variables," *Nature* **431**
3. W. P. Bowen, N. Treps, B. C. Buchler, R. Schnabel, T. C. Ralph, Hans-A. Bachor, T. Symul, and P. K. Lam, "Experimental investigation of continuous-variable quantum teleportation," *Phys. Rev. A* **67**, 032302 (2003).
4. X. Y. Li, Q. Pan, J. T. Jing, J. Zhang, C. D. Xie, and K. C. Peng, "Quantum Dense Coding Exploiting a Bright Einstein-Podolsky-Rosen Beam," *Phys. Rev. Lett.* **88**, 047904 (2002).
5. J. T. Jing, J. Zhang, Y. Yan, F. G. Zhao, C. D. Xie, and K. C. Peng, "Experimental Demonstration of Tripartite Entanglement and Controlled Dense Coding for Continuous Variables," *Phys. Rev. Lett.* **90**, 167903 (2003).
6. X. J. Jia, X. L. Su, Q. Pan, J. R. Gao, C. D. Xie, and K. C. Peng, "Experimental Demonstration of Unconditional Entanglement Swapping for Continuous Variables," *Phys. Rev. Lett.* **93**, 250503 (2004).
7. K. Bencheikh, T. Symul, A. Jankovic, and J. A. Levenson, "Quantum key distribution with continuous variables," *J. Mod. Opt.* **48**, 1903–1920 (2001).
8. X. Su, W. Wang, Y. Wang, X. Jia, C. Xie, and K. Peng, "Continuous variable quantum key distribution based on optical entangled states without signal modulation," *Europhys. Lett.* **87**, 2000–2005 (2009).
9. N. C. Menicucci, P. van Loock, M. Gu, C. Weedbrook, T. C. Ralph, and M. A. Nielsen, "Universal Quantum Computation with Continuous-Variable Cluster States," *Phys. Rev. Lett.* **97**, 110501 (2006).
10. A. H. Tan, Y. Wang, X. L. Jin, X. L. Su, X. J. Jia, J. Zhang, C. D. Xie, and K. C. Peng, "Experimental generation of genuine four-partite entangled states with total three-party correlation for continuous variables," *Phys. Rev. A* **78**, 013828 (2008).
11. J. Yoshikawa, Y. Miwa, A. Huck, U. L. Andersen, P. van Loock, and A. Furusawa, "Demonstration of a Quantum Nondemolition Sum Gate," *Phys. Rev. Lett.* **101**, 250501 (2008).
12. A. Furusawa, and N. Takei, "Quantum teleportation for continuous variables and related quantum information processing," *Phys. Rep.* **443**, 97–119 (2007).

13. S. F. Pereira, K. C. Peng, and H. J. Kimble, "Squeezed state generation and nonclassical correlations in nondegenerate parametric down conversion," in *Coherence and Quantum Optics VI*, J. H. Eberly, L. Mandel and E. Wolf, eds. (Plenum, New York, 1990) pp. 889–890
14. Z. Y. Ou, S. F. Pereira, H. J. Kimble, and K. C. Peng, "Realization of the Einstein-Podolsky-Rosen paradox for continuous variables," *Phys. Rev. Lett.* **68**, 3663 (1992).
15. Y. Zhang, H. Wang, X. Y. Li, J. T. Jing, C. D. Xie, and K. C. Peng, "Experimental generation of bright two-mode quadrature squeezed light from a narrow-band nondegenerate optical parametric amplifier," *Phys. Rev. A* **62**, 023813 (2000).
16. W. P. Bowen, R. Schnabel, P. K. Lam, and T. C. Ralph, "Experimental Investigation of Criteria for Continuous-Variable Entanglement," *Phys. Rev. Lett.* **90**, 043601 (2003).
17. J. Laurat, T. Coudreau, G. Keller, N. Treps, and C. Fabre, "Effects of mode coupling on the generation of quadrature Einstein-Podolsky-Rosen entanglement in a type-II optical parametric oscillator below threshold," *Phys. Rev. A* **71**, 022313 (2005).
18. A. S. Villar, L. S. Cruz, K. N. Cassemiro, M. Martinelli, and P. Nussenzveig, "Generation of bright two-color continuous variable entanglement," *Phys. Rev. Lett.* **95**, 243603 (2005).
19. X. Su, A. Tan, X. Jia, Q. Pan, C. Xie, and K. Peng, "Experimental demonstration of quantum entanglement between frequency-nondegenerate optical twin beams," *Opt. Lett.* **31**
20. J. T. Jing, S. Feng, R. Bloomer, and O. Pfister, "Experimental continuous-variable entanglement of phase-locked bright optical beams," *Phys. Rev. A* **74**, 041804 (2006).
21. Y. Takeno, M. Yukawa, H. Yonezawa, and A. Furusawa, "Observation of -9 dB quadrature squeezing with improvement of phase stability in homodyne measurement," *Opt. Express* **15**, 4321–4327 (2007). <http://www.opticsinfobase.org/oe/abstract.cfm?URI=oe-15-7-4321>
22. H. Vahlbruch, M. Mehmet, S. Chelkowski, B. Hage, A. Franzen, N. Lastzka, S. Gößler, K. Danzmann, and R. Schnabel, "Observation of Squeezed Light with 10-dB Quantum-Noise Reduction," *Phys. Rev. Lett.* **100**, 033602 (2008).
23. M. Yukawa, R. Ukai, P. van Loock, and A. Furusawa, "Experimental generation of four-mode continuous-variable cluster states," *Phys. Rev. A* **78**, 012301 (2008).
24. R. W. P. Drever, J. L. Hall, F. V. Kowalski, J. Hough, G. M. Ford, A. J. Munley, and H. Ward, "Laser phase and frequency stabilization using an optical resonator," *Appl. Phys. B: Photophys. Laser Chem.* **31**, 97–105 (1983).
25. J. Zhang and K. C. Peng, "Quantum teleportation and dense coding by means of bright amplitude-squeezed light and direct measurement of a Bell state," *Phys. Rev. A* **62**, 064302 (2000).
26. Lu-Ming Duan, G. Giedke, J. I. Cirac, and P. Zoller, "Inseparability Criterion for Continuous Variable Systems," *Phys. Rev. Lett.* **84**, 2722 (2000).
27. P. T. Cochrane, T. C. Ralph, and G. J. Milburn, "Teleportation improvement by conditional measurements on the two-mode squeezed vacuum," *Phys. Rev. A* **65**, 062306 (2002).

1. Introduction

Continuous variable (CV) quantum entanglement between amplitude and phase quadratures of optical fields has been intensively investigated. The optical CV entangled states have been utilized in quantum information science to realize deterministic quantum teleportation of coherent states [1, 2, 3], unconditional dense coding quantum communication [4, 5], entanglement swapping [6], quantum key distribution [7, 8], and so on. Recently, it has been proved that CV entanglement can be applied to develop quantum computation and universal quantum information process [9, 10, 11, 12].

At the beginning of 1990s, Kimble's group experimentally generated a pair of CV entangled optical beams by type-II down-conversion in a subthreshold nondegenerate optical parametric amplifier (NOPA) and demonstrated the Einstein-Podolsky-Rosen (EPR) paradox firstly in CV regime [13, 14]. The quantum correlations of amplitude and phase quadratures between output signal and idler beams observed in their experiment were 3.6 ± 0.2 dB below the quantum noise limit (QNL) normalized to the vacuum noise of the corresponding optical field. Almost ten years later, the bright EPR entangled beams with ~ 4 dB amplitude (phase) correlation and phase (amplitude) anticorrelation were generated from a NOPA with injected signals operating at amplification (deamplification) [4, 15, 16, 17]. Intense EPR entangled beams were produced from optical parametric oscillators (OPOs) operating above threshold by several groups recently [18, 19, 20]. However, the quadrature-phase correlations of these intense beams were worse than that obtained from NOPAs below threshold. Another efficiently and extensively

used scheme generating CV entangled states is to interfere two single-mode squeezed beams on a 1 : 1 beamsplitter [1, 2]. The two squeezed beams should have identical frequency to achieve stable interference. In these experiments, they were produced from two degenerate optical parametric amplifiers (DOPAs) with identical type-I nonlinear crystal pumped by a laser to ensure their optical frequency being the same. Recent years, the single-mode squeezed light beams of ~ 9 dB and ~ 10 dB were generated from a DOPA with a PPKTP (periodically poled KTiOPO_4) crystal and a monolithic DOPA made by $\text{MgO}:\text{LiNbO}_3$ crystal, respectively, based on some technical improvements [21, 22]. It is exciting that CV four-mode cluster states with the multi-mode quadrature correlations of ~ 6 dB below the QNL have been experimentally observed recently [23]. In the system of Ref. [23], the four initial single-mode squeezed states were generated from four DOPOs pumped by a Ti:sapphire laser. However, the correlations of EPR beams from NOPAs still keep at ~ 4 dB so far. Under the motivation of the great achievement on DOPAs, we followed the ideas in Ref. [21, 22] to implement some technical improvements on the system for EPR entangled state generation from a NOPA. At first, the amplitude and phase noises of the pump laser of the NOPA were reduced to the QNL level by using a specifically designed mode cleaner (MC). Second, the phase fluctuations in all phase locking systems were controlled detailedly. Based on above improvements the quantum correlations of quadrature components between EPR entangled beams generated from a NOPA were increased from ~ 4 dB to ~ 6 dB below the QNL. The experiment results show that there is potential to further enhance the CV entanglement of output optical beams from NOPAs.

2. Experimental setup

The schematic of the EPR entangled state generation system is shown in Figure 1. The laser is a continuous wave intra-cavity frequency-doubled and frequency stabilized Nd:YAP/KTP (Nd-doped YAIO_3 perovskite / potassium titanyl phosphate) laser (Yuguang Co. Ltd., F-VIB). The harmonic wave of 2 W at 540 nm and the fundamental wave of 0.8 W at 1080 nm are generated simultaneously from the laser. The output green and infrared lasers are separated by a mirror coating with high reflectivity for 540 nm and high transmission for 1080 nm, and then are used as the pump field and the injected signal of the NOPA, respectively. The traveling-wave resonator placed in the laser beam of 1080 nm serves as the optical low-pass filter of noises and the spatial mode cleaner (MC1). The finesse and the linewidth of MC1 for 1080 nm are 700 and 1 MHz, respectively. An important improvement with respect to our previously experimental system [4, 15] is that a mode cleaner (MC2) with a finesse of 1000 and linewidth of 600 kHz for 540 nm is added in the pump laser before the NOPA. MC2 is also a traveling-wave resonator consisting of three mirrors with the total cavity length of 520 mm. Both MC1 and MC2 are temperature-controlled to improve the mechanic stability. The MC2 is adjusted to resonating with the second harmonic laser field via a Pound-Drever-Hall locking scheme with a phase modulation frequency at 5.8 MHz [24]. We found that MC2 not only can significantly improve the quality of spatial distribution of the pump laser but also can reduce its phase fluctuation.

The NOPA consists of an α -cut type-II KTP ($3 \times 3 \times 10 \text{ mm}^3$) crystal and a concave mirror. The front face of KTP is coated to be used as the input coupler (the transmission 99.8% at 540 nm wavelength and 0.04% at 1080 nm) and the other face of which is coated with the dual-band antireflection at both 540 nm and 1080 nm. A concave mirror of 50 mm curvature radius, which is coated with transmission $T = 5.2\%$ at 1080 nm and high reflectivity at 540 nm, is used as the output coupler of the EPR beams at 1080 nm. The measured finesse at 1080 nm is 117, so the intra-cavity loss is $L = 0.17\%$. The cavity length of the NOPA is 54 mm and the waist size radius of the infrared field at the input face of KTP crystal is approximately $38 \mu\text{m}$. The concave mirror is mounted on a piezoelectric transducer (PZT) for locking actively the cavity length of NOPA on resonance with the injected signal at 1080 nm via a Pound-Drever-Hall locking scheme with

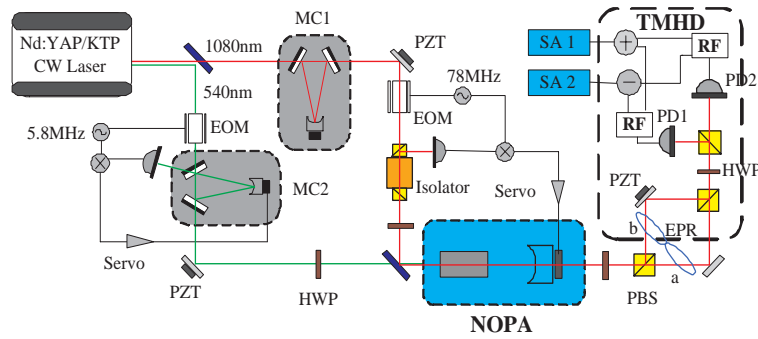


Fig. 1. (Color online) Schematic of the experimental setup. MC1-2: mode cleaner, PZT: piezoelectric transducer, Servo: servo amplifier circuit for feedback system, EOM: electro-optical modulator, HWP: half wave-plate, NOPA: nondegenerate optical parametric amplifier, PBS: polarization beamsplitter, TMHD: two-mode homodyne detector for continuous variable entanglement, PD1-2: photodiode detector (ETX500 InGaAs), RF: radio frequency power splitter, \oplus : positive power combiner; \ominus : negative power combiner, SAs: spectrum analyzers.

the phase modulation frequency of 78 MHz [24]. The temperature of KTP crystal are carefully controlled at 63°C to satisfy the type-II phase match condition. Through a parametric down conversion process of type-II phase match, a bright EPR beam with anticorrelated amplitude quadratures and correlated phase quadratures can be produced from a NOPA operating in the state of deamplification, where the relative phase between pump field and the injected signal is locked to π [4]. The correlation variances of amplitude (\hat{X}) and phase (\hat{Y}) quadratures of the two EPR beams \hat{a} and \hat{b} are given by $\langle \delta^2(\hat{X}_a + \hat{X}_b) \rangle = \langle \delta^2(\hat{Y}_a - \hat{Y}_b) \rangle = 2e^{-2r}$, where r is the correlation parameter which depends on the strength and the time of parametric interaction in NOPA [8]. The values of $r = 0$ and $r \rightarrow +\infty$ correspond to no correlation and ideal correlation, respectively. The EPR beams, which have identical frequency with the injected signal and the orthogonal polarization with each other, are separated by a polarization beam splitter (PBS). The quantum correlations between amplitude and phase quadratures of the two EPR beams are measured by a two-mode homodyne detector (TMHD) for continuous variable entanglement [25], which consists of two PBS, a half wave-plate (HWP), two ETX-500 photodiode detectors (PD1 and PD2) and two radio frequency power splitters (RFs). The detector requires to combine the two entangled optical modes on a beamsplitter, thus it is not able to be used for verifying the entanglement of two spatially separated modes and also can not be applied in the measurement of the squeezed vacuum states due to that it can only work with bright signal and idler beams. Using a PZT placed in one of the detected two beams, we lock the relative phase between two EPR beams to $\pi/2$. The output photo-currents from the radio frequency power splitter are combined by the positive power combiner (\oplus) and the negative power combiner (\ominus) to obtain the noise powers of amplitude sum and phase difference, respectively. Then they are recorded by spectrum analyzers 1 and 2, respectively. To determine the corresponding QNL, we blocked the pump field of NOPA and locked the NOPA to resonate with the injected seed light. Adjusting the power of the injected seed light to make the intensity of the output coherent state at 1080 nm exactly equals that of the generated entangled state, in this case the measured variances are the corresponding QNL.

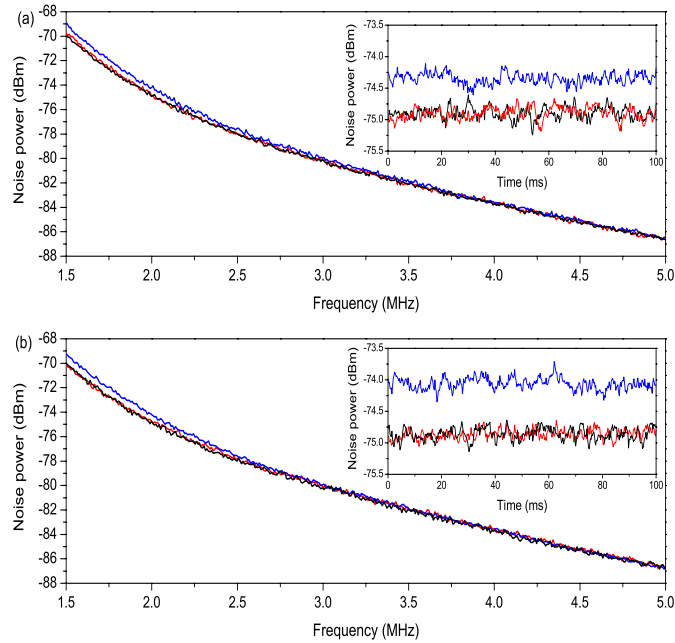


Fig. 2. (Color online) The measured noise powers of amplitude (a) and phase (b) quadratures of pump laser. Black lines: QNL, red lines: noise of pump laser with MC2, blue lines: noise of pump laser without MC2. Insets: the noises of amplitude (a) and phase (b) quadratures at 2 MHz. The parameter of spectrum analyzer: RBW: 30 kHz, VBW: 100 Hz.

3. Experimental results and discussion

To analyze the effect of the pump noises we measured the amplitude and phase noise power spectra of the pump laser at 540 nm with and without the use of MC2, which are shown in Fig. 2(a) and (b) respectively. The amplitude (a) and the phase (b) noises in Fig. 2 were measured by another balanced homodyne system, which is not shown in Fig. 1. The used laser powers for the local oscillation beam and the signal beam for the homodyne measurement are 5.7 mW and 30 μ W, respectively. The measurements for both cases with and without the use of MC2 were implemented before NOPA. The photodiode used in the balanced homodyne system is S5973-02 (Hamamatsu). In the measurements, the noises of the used local beams have been filtered to the QNL and the resolution bandwidth (RBW) and video bandwidth (VBW) are 30 kHz and 100 Hz, respectively. In Fig. 2, the black, red and blue lines correspond to the QNL, the noise power of the output coherent state with and without the use of MC2, respectively. We can see that if MC2 is not used both amplitude and phase noises are higher than the QNL from 1.5 MHz to 4 MHz. These excess noise in the pump laser come from the relaxation oscillation of laser and they decrease along with the increase of the analysis frequency gradually to the QNL after 4 MHz. The noise levels of amplitude and phase quadratures of the pump laser are 0.5 dB and 1 dB above the QNL at 2 MHz, respectively [see the insets in Fig. 2(a) and (b)]. After the use of MC2, the amplitude and phase noises are reduced to the QNL at 2 MHz, where

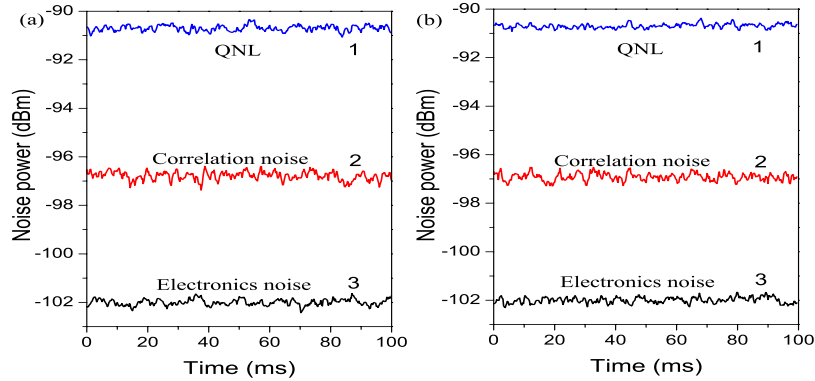


Fig. 3. (Color online) The measured noise powers of amplitude sum (a) and phase difference (b) at 2 MHz. The parameter of spectrum analyzer: RBW: 30 kHz, VBW: 100 Hz.

the correlation variances will be measured.

It has been proved that the relative phase fluctuations in homodyne measurement significantly influence the measured correlations [21]. To reduce the relative phase fluctuations the stack PZT (Piezomechanik GmbH, HPSt) is chosen and the electronic feedback system is optimized. At first, the modulation frequency and the modulation depth are adjusted to give an error signal with higher signal-to-noise ratio. Then a low noise highvoltage amplifier (Yuguang Co. Ltd. YG2009A-350V) with a lower output voltage noise of 6 mV_{pp} is used for amplifying the error signal. After these improvements, the phase fluctuation of the phase locking system reach 1.8° .

To produce the entangled states of light with anticorrelated amplitude quadratures and correlated phase quadratures, the NOPA is pumped with a green laser of 170 mW which is 60 mW below the oscillation threshold of 230 mW and is operated at deamplification [4, 15]. In this case, the intensity of the output EPR entangled beams is $\sim 80 \mu\text{W}$ and the parametric gain is $g = 25$. The escape efficiency and the cavity linewidth of the NOPA are $\eta_{esc} = T/(T+L) = 96.8\%$ and $\Delta\nu = 23.7 \text{ MHz}$, respectively. The detection efficiency and the mode-matching efficiency of the detection system are 90% and 99.9%, respectively.

The measured noise powers of the amplitude sum (a) and the phase difference (b) of the generated EPR beams are shown in Fig. 3. Pairs of QNLs, correlated noise and electronic noise are measured simultaneously by two spectrum analyzers with the following parameters: measurement frequency of 2 MHz in zero span mode, RBW of 30 kHz, and VBW of 100 Hz. Trace (1) is the QNL, which corresponds to the noise level of coherent state with a power of $80 \mu\text{W}$. Traces (2) in Fig. 3(a) and (b) are the measured correlation variances of the amplitude sum $\langle \delta^2(\hat{X}_a + \hat{X}_b) \rangle$ and the phase difference $\langle \delta^2(\hat{Y}_a - \hat{Y}_b) \rangle$ respectively, which are $6.08 \pm 0.18 \text{ dB}$ and $6.22 \pm 0.16 \text{ dB}$ below the corresponding QNL. The electronic noise of detector [trace (3)] is approximately 11 dB below the QNL. Considering the influence of electronics noise, the actual quantum correlation should be $\langle \delta^2(\hat{X}_a + \hat{X}_b) \rangle = 7.30 \pm 0.18 \text{ dB}$ and $\langle \delta^2(\hat{Y}_a - \hat{Y}_b) \rangle = 7.50 \pm 0.16 \text{ dB}$ below the corresponding QNL. The generated bright EPR entangled beams satisfy the inseparable criteria [26]: $\langle \delta^2(\hat{X}_a + \hat{X}_b) \rangle + \langle \delta^2(\hat{Y}_a - \hat{Y}_b) \rangle = 0.485 < 2$, which corresponds to the observed entanglement of 6 dB without subtracting electronics noise.

In most theoretical discussions the noises of the pump lasers of NOPA are assumed at the QNL without excess noises. However, in practical cases the excess noises usually exist in the

pump lasers which will enter in the output fields of NOPA during the parametric conversion and thus decrease its entanglement. Of course, the factors limiting entanglement in NOPA devices are of variety. Generally, the entanglement from NOPA are mainly limited by the quality of nonlinear crystal (nonlinear coefficient and losses), escape efficiency and cavity linewidth of NOPA, detection efficiency, mode-matching efficiency of detection system, and phase fluctuation of phase locking system [21]. Towards further increasing the entanglement for our system, the currently limiting factors mainly are the lower escape efficiency of the optical cavity of the NOPA and the lower detection efficiency of the detection system. If we increase the escape efficiency from present 96.8% to 98.6% ($T = 12\%$) and the detection efficiency from present 90% to 99%, over 10 dB entanglement will be expected. Besides, observing high entanglement the electronic noise background of the detection system has to be reduced to a large extent, for that the present TMHD should be replaced by the normal balanced homodyne detector [14]. At last, we should mention that the infinite entanglement can not be obtained because it requires infinite energy [27].

4. Conclusion

For the conclusion, we obtained CV optical entangled states with amplitude and phase quadrature quantum correlations of ~ 6 dB, which are the highest correlations generated from NOPA devices so far to the best of our knowledge. Comparing with our previous NOPA systems [4, 15], two technical improvements are made: 1. Both amplitude and phase noises of the pump laser of NOPA are reduced to the QNL level with a suitable mode cleaner. 2. The relative phase fluctuations of phase locking systems are minimized. Our experiment shows that the implementation of NOPAs on entanglement generation can be significantly enhanced by means of some technical improvements on the pump laser and the phase locking systems even using the same NOPA configuration and nonlinear crystal.

Acknowledgments

This research was supported by the NSFC (Grants No. 60736040 and 10804065), NSFC Project for Excellent Research Team (Grant No. 60821004), National Basic Research Program of China (Grant No. 2007BAQ03918).